Infrared Multiple Photon Dissociation in the Quadrupole Ion Trap Via a Multipass Optical Arrangement

James L. Stephenson, Jr., Matthew M. Booth, Joseph A. Shalosky, John R. Eyler, and Richard A. Yost
Department of Chemistry, University of Florida, Gainesville, Florida, USA

The design of a novel multipass optical arrangement for use with infrared multiple photon dissociation (IRMPD) in the quadrupole ion trap is presented. This design circumvents previous problems of limited IR laser power, small IR absorption cross sections for many molecules, and the limited ion statistics of trapping and detection of ions for IRMPD in the quadrupole ion trap. In contrast to previous designs that utilized the quadrupole ion store, the quadrupole ion trap was operated in the mass selective instability mode with concurrent resonance ejection. The instrumental design consisted of a modified ring electrode with three spherical concave mirrors mounted on the inner surface of the ring. This modified design allowed for eight laser passes across the radial plane of the ring electrode. IRMPD of protonated bis(2-methoxyethyl)ether (diglyme) was used to characterize the performance of the multipass ring electrode. Two consecutive reactions for the IRMPD of protonated diglyme were observed with a lower energy channel predominant at less than 0.6 J (irradiation times from 1 to 30 ms) and a second channel predominant at energies greater than 0.6 J (irradiation times > 30 ms). Other studies presented include a discussion of the dissociation kinetics of protonated diglyme, the use of a pulsed valve for increased trapping efficiency of parent ion populations, and the effects of laser wavelength and of ion residence time in the radial plane of the ring electrode on photodissociation efficiency. *(J Am Soc Mass Spectrom 1994, 5, 886–893)*

Over the past 15 years photodissociation has become an integral tool in the study of gas-phase ion chemistry [1, 2]. The combination of mass spectrometry (employing both ion trap and ion cyclotron resonance instruments) and photodissociation has been used successfully to investigate the chemical kinetics, reactivity, and spectroscopy of various ionic species [3–9]. The long storage times and instrumental configuration of trapping instruments are ideally suited for photodissociation experiments. Some capabilities of trapping instruments include the measurement of photon-induced ion decay as a function of laser irradiance time, the use of the multiphoton absorption process to study fragmentation, and the use of the photodissociation spectrum as a fingerprint for determination of isomeric ion structures [10].

Infrared multiple photon dissociation (IRMPD) is particularly well suited for use with trapping instruments. The ability to trap ions for an extended period of time at low pressures in both the ion cyclotron resonance (ICR) cell and the quadrupole ion trap mass spectrometer (QITMS) allows for the sequential absorption of infrared photons via low intensity continuous-wave (cw) infrared radiation. The IRMPD process was first characterized by Beauchamp and co-workers [11, 12] for positive ions in the ICR cell. The first successful use of the quadrupole ion trap in conjunction with IRMPD involved study of the proton-bound dimer of 2-propanol utilizing a cw CO_2 laser [13, 14]. The instrumental configuration consisted of a quadrupole ion store (QUISTOR) connected directly to the ion source of a quadrupole mass filter. Optimization of this instrumental configuration for photodissociation studies of proton-bound dimers was reported by Hughes et al. [15]. The same experimental apparatus has been employed to investigate the gas-phase ion chemistry of ethanethiol, 1- and 2-propanethiol, and 1-hydroxyethanethiol [16, 17].

All earlier studies of the IRMPD process in the ion trap were performed with a single-pass ring electrode design, with a 3-mm-diameter hole on the center axis of the ring electrode as the entrance aperture for the low power cw CO_2 laser beam. Upon reaching the other side of the ring electrode, a portion of the beam passed through a 0.8-mm-diameter hole and through a NaCl window, where the laser power was monitored externally. The remainder of the laser beam was re-

Address reprint requests to Dr. Richard A. Yost, University of Florida, Department of Chemistry, P.O. Box 117200, Gainesville, FL 32611-7200.

1044-0305/94/$7.00

Received November 2, 1993
Revised May 13, 1994
Accepted May 16, 1994

flected by the ring electrode throughout the QUISTOR [13].

The ability to determine the dissociation pathway of lowest activation energy is a major advantage of IRMPD for well relaxed ions. This procedure can be used to simplify the structural elucidation process. However, to take full advantage of the slow multiphoton absorption process, the rate of photon absorption must exceed the sum of all radiative and collisional relaxation rates. For many compounds, absorption cross sections in the IR region are very low, and a method is needed to increase the optical path length and photodissociation efficiency. In addition, because of both the limited tunability of the standard IR laser sources (CO_2, CO, NO) and the low power of these lasers, there has been no systematic attempt to use IRMPD to obtain gaseous ion spectra and structural information.

In our laboratory, a multipass optical arrangement was constructed to produce eight laser passes across the radial plane of the ion trap ring electrode. This modified optical arrangement, as originally described by White [18], increased the optical path length and thus the amount of photon absorption obtained in the IR region. Incorporation of this novel White-type cell design into an ICR cell was first demonstrated by Watson et al. [19]. The White-type ICR cell was used for the study of resonance-enhanced two-laser infrared multiphoton dissociation of gaseous perfluoropropene cations [19], gallium hexafluoroacetylacetonate anions [18, 19], protonated diglyme cations [19, 20], and allyl bromide cations [20]. The authors reported that fragmentation in the White-type cell (by using energies lower by almost a factor of 20) was comparable to that seen in a simple double-pass experiment.

In this report, we discuss characterization of a novel multipass optical arrangement for use in a quadrupole ion trap. A detailed investigation into the IRMPD of protonated diglyme, including photon absorption, first-order dissociation kinetics, and wavelength dependence, is presented. In addition, a pulsed-valve technique is introduced that allows for the efficient trapping of parent ion populations, with subsequent collision-free conditions needed to study slow multiphoton dissociation processes. Finally, preliminary results are presented for the effect of Mathieu parameters q_z and a_z on photodissociation efficiency.

Experimental

All experiments were performed on a Finnigan MAT (San Jose, CA) ion trap mass spectrometer (ITMS). Except for the pulsed-valve experiments, the ion trap was operated with no He buffer gas in the vacuum chamber. The base pressure of the instrument was 3.5×10^{-8} torr (uncorrected), as indicated on an ion gauge mounted on the vacuum manifold. The Teflon® ring electrode spacers were found to absorb strongly at 944 cm^{-1} during the laser irradiation period, which desorbed both neutral and ionic species that can affect

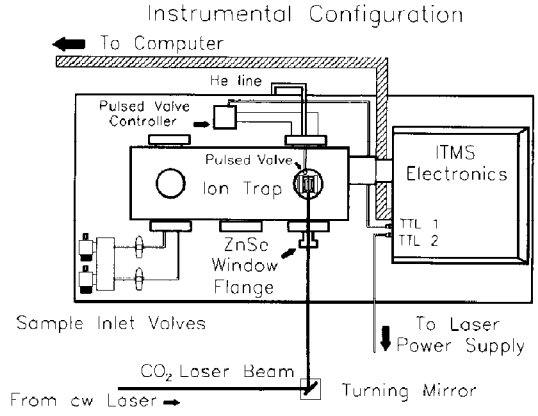

Figure 1. Instrumental configuration for IRMPD in the ion trap.

both ion storage efficiency and detection; they were therefore removed. The vacuum manifold was equipped with a modified flange containing a ZnSe window to pass IR radiation. The software used was modified to accommodate two TTL pulses for computer control of both the cw CO_2 laser and the pulsed-valve apparatus [21]. The experimental arrangement can be seen in Figure 1.

The cw CO_2 laser employed was an Apollo Model 570 that is line-tunable over a wavelength range of 1099–924 cm^{-1} and has a beam size of approximately 1.0 cm. The maximum laser power obtainable was 50 W at 944 cm^{-1}. The laser power supply was modified with electronics that transformed an incoming TTL signal to the CMOS logic used by the laser. A spectrum analyzer (Optical Engineering, Model 16-A, Santa Rosa, CA) was placed directly in-line with the cw CO_2 laser beam for wavelength measurements. All laser energy measurements (Coherent Radiation Model 410 power meter, Boulder, CO) were taken inside the ITMS vacuum manifold to correct for beam loss at the turning mirror surface and ZnSe window. Because of space considerations, the ion trap analyzer was removed from the ITMS vacuum manifold for the energy measurements. The power meter was then positioned exactly at the location where the laser beam would enter the ion trap analyzer. The laser was placed parallel to the ITMS manifold with the beam reflected at a 90° angle by a silver-coated mirror as seen in Figure 1. Laser beam alignment was accomplished with a He–Ne laser placed in-line with the cw CO_2 laser. The analyzer of the ITMS was fitted with a modified mounting bracket to allow for rotation of the ion trap analyzer from its original fixed position to facilitate alignment.

The 1.0-cm-diameter IR laser beam was attenuated by the 0.3-cm (1/8-in.) entrance aperture on the ring electrode. The ring electrode was modified by incorporation of three polished stainless steel spherical concave mirrors (radius of curvature = 2.0 cm) mounted on the inner surface of the ring, as shown in Figure 2. The approximate photon density (assuming constant

intensity across the attenuated beam width) observed in the radial plane of the ring electrode can be seen in Figure 2. The most critical adjustment of the mirror system was the separation of the centers of curvature of the mirrors A and B shown in Figure 2. This separation determines the number of beam transversals across the ring electrode: 4, 8, 12, or any other multiple of 4. The mirrors were mounted on the ring electrode such that the centers of curvature of mirrors A and B were on the front surface of mirror C, and the center of curvature of mirror C was halfway between mirrors A and B [18].

Each mirror (and its mounting bracket) was constructed from a single piece of stainless steel. At one end of each piece, the radius of curvature was cut (r = 2.0 cm) and the surface was highly polished. The three mirrors were mounted into precision-drilled holes in the ring electrode positioned such that the alignment was automatic; no realignment has been needed since the original assembly of the multipass ring electrode (19 months). A small mechanical screw was used to hold each mirror–mirror mount assembly in place on the ring electrode. Laser alignment was set such that the center portion of the 1-cm Gaussian beam profile was transmitted through the entrance aperture, thus yielding high photodissociation efficiency. Therefore with efficiencies already greater than those published for previous designs on a QUISTOR trap or ICR cell, condensing the beam down to 0.3 cm was considered less important than examining the numerous ways in which gas-phase ion chemistry can be studied via IRMPD with this unique design. Furthermore, with the beam focused to 0.3 cm, damage to the surface of the ion trap mirror was observed when the laser was tuned to a strong IR emission line (e.g., 10.59 μm). With continued use over a 19-month period, no degradation of the ion trap mirror surfaces has been observed with the unfocused laser beam.

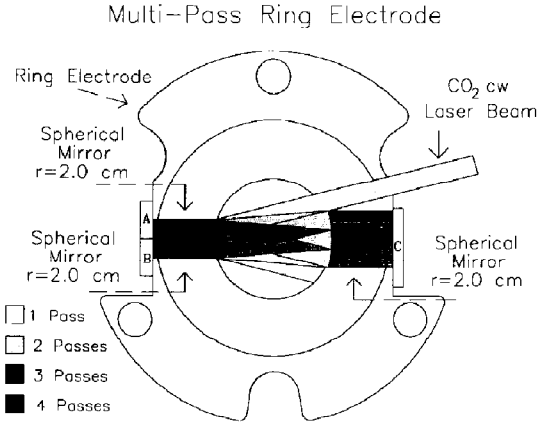

Figure 2. Modified ring electrode for multipass IRMPD experiments. Mirror positions and the eight passes across the radial plane of the ring electrode, along with approximate photon density in the radial plane of the ring electrode, are shown. The positions of mirrors A and B determine the number of laser transversals across the radial plane of the ring electrode.

The pulsed valve used in the experiments (Series 9, General Valve Corporation, Fairfield, NJ) was mounted on the opposite flange from the ZnSe window (see Figure 1) and was used to pulse He into the ion trap to increase trapping efficiency. The pulsed valve was placed 0.5 cm from the outer diameter of the ring electrode. Its horizontal position was between the modified ring electrode and the entrance endcap. The pulsed-valve controller (built at the University of Florida) was controlled by an external TTL pulse generated by the ITMS electronics. The timing diagram shown in Figure 3 displays both the laser control TTL pulse and the pulsed valve TTL control pulse for a given scan function.

Bis(2-methoxyethyl)ether (diglyme; ACS reagent grade purchased from Fisher Scientific, Fairlawn, NJ) was introduced via a Granville-Phillips (Boulder, CO) fine metering valve directly into the ion trap manifold. Depending on the experiment, the diglyme sample pressure ranged from 1.1 to 3.6 $\times$ 10^{-7} torr. Formation of the protonated diglyme was accomplished by chemical self-ionization, predominantly due to the reaction of the low mass even-electron fragment ions from electron ionization (EI) of diglyme with the neutral diglyme molecules for 400 ms. The resulting $[M + H]^+$ ion of diglyme was then mass isolated by a two-step rf/dc isolation routine [22]. Next a 400-ms delay was included to allow for removal of any excess internal energy by radiative and/or collisional cooling. The protonated diglyme was then irradiated for a specified time period with the cw CO_2 laser. After the laser irradiation period, a 10-ms time period was incorporated for decay of the laser output when the high voltage was turned off. For all photodissociation efficiency measurements in this report, the m/z 103 product ion from the IRMPD of protonated diglyme was resonantly ejected (q_z = 0.3, frequency = 115.6 kHz,

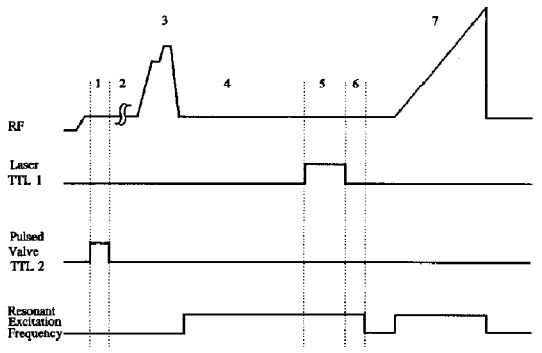

Figure 3. ITMS scan function and timing diagram for a typical IRMPD experiment (figure not to scale). 1, pre-ionization/pulsed valve on; 2, ionization–chemical self-ionization reaction; 3, two-step mass isolation; 4, vibrational relaxation; 5, laser on; 6, laser decay; 7, acquisition.

amplitude = 100 mV) both during the laser irradiation period and during the laser decay period (periods 5 and 6 in Figure 3). This prevented the possible occurrence of any ion–molecule reactions as the result of the reaction of the sequential absorption product (m/z 59) with neutral diglyme. The resulting photofragments were then mass analyzed via resonance ejection with $q_{z\ \mathrm{eject}} = 0.89$ and an amplitude of 1.5 V (zero to peak) [23, 24].

Results and Discussion

Figure 4a shows the EI mass spectrum of diglyme at a sample pressure of 3.6×10^{-7} torr. Typically no molecular ion $M^{+\cdot}$ at m/z 134 is present. Instead fragment ion m/z 89, formed by cleavage of the carbon–carbon bond, and fragment ion m/z 59, formed by either loss of aldehyde from m/z 89 or loss of $C_3H_7O_2$ from the molecular ion, dominate the EI mass spectrum. The inability to form the molecular ion, coupled with the ability to produce protonated diglyme (m/z 135) easily via ion–molecule reactions, led to the use of the protonated molecule for IRMPD studies.

In Figure 5, the wavelength dependence of the IRMPD spectrum of protonated diglyme is shown. The wavelength was varied from 933 to 953 cm^{-1}. The spectrum was normalized to an irradiation energy of 0.2520 J. The reaction channel was not found to depend on the laser wavelength used; only the photodissociation efficiency was affected by varying the laser wavelength. The maximum photodissociation efficiency was found at 944 cm^{-1}. A higher degree of photodissociation efficiency was observed in the ion trap compared to an eight-pass ICR cell ($\cong$90% at λ_{max} versus $\cong$55% at λ_{max}). The difference in these values was attributed to the easier alignment of the ion trap system. The width of the absorption peak for protonated diglyme in the ICR cell was approximately 7 cm^{-1} [19] compared to 12 cm^{-1} for the ion trap. This difference may arise from the deviation in ion temperatures in the QITMS compared to those in the ICR. Ion translational temperatures (measured with argon–nitrogen kinetic thermometer reactions) in the QITMS were found to lie in the range 1700–3300 K, whereas those in the ICR were found to be 500–880 K [25, 26]. The higher kinetic energy of the ions in the QITMS may correlate with a higher internal energy content, and this lead to a larger absorption bandwidth because of a higher percentage of molecules in the vibrational quasicontinuum.

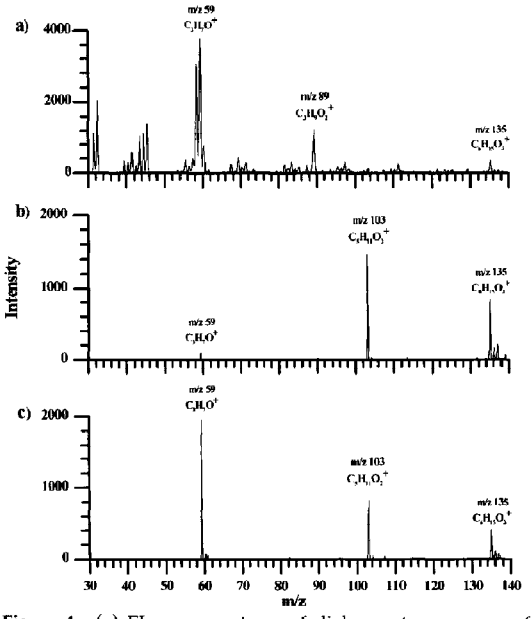

Figure 4. (a) EI mass spectrum of diglyme at a pressure of 3.6×10^{-7} torr and 15-ms ionization time (no He present). (b) IRMPD spectrum of protonated diglyme at 944 cm^{-1} and 10-ms irradiance time (energy = 0.201 J). (c) IRMPD spectrum of protonated diglyme at 944 cm^{-1} and 40-ms irradiance time (energy = 0.852 J).

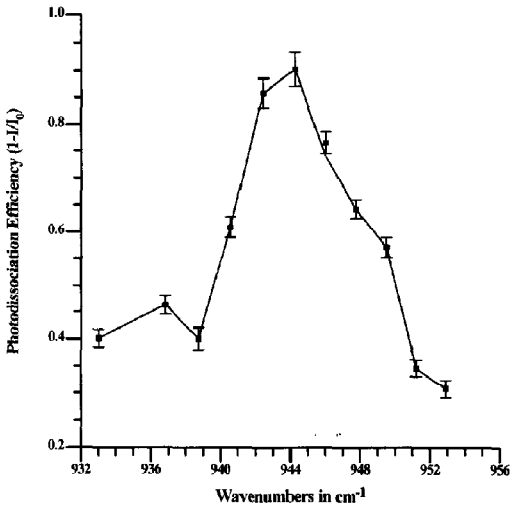

Figure 5. Photodissociation efficiency as a function of laser wavelength for protonated diglyme at an energy of 0.252 J (1.1×10^{-7} torr diglyme).

Characteristic photodissociation spectra of the $[M + H]^+$ ion of diglyme at 944 cm^{-1} are shown in Figure 4b and c. At lower irradiation energies (irradiation time = 10 ms) the single reaction channel observed was the formation of m/z 103 with corresponding loss of neutral methanol as shown in Figure 4b. At higher irradiation energies (irradiation time = 40 ms) the dominant reaction channel involved the loss of an acetaldehyde neutral from the m/z 103 ion shown in Figure 4c. The presence of a small m/z 59 peak at lower irradiance times suggested a competitive reaction mechanism for the formation of the product ion species from the m/z 135 parent ion. Alternatively, when ion intensity was plotted as a function of laser irradiance time (Figure 6), the appearance was that of a series of consecutive reactions.

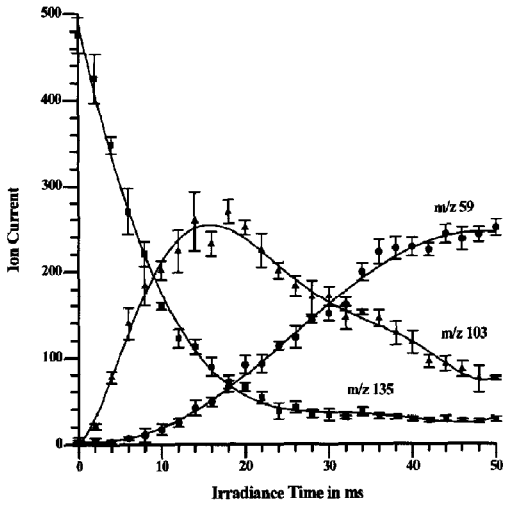

Figure 6. IRMPD ion growth curves that show the two reaction channels for protonated diglyme.

To determine if the reaction mechanism was competitive or consecutive, a series of MS^n experiments was conducted. In the first experiment, the formation and mass isolation of protonated diglyme (m/z 135) were achieved as described earlier. A tandem mass spectrometry experiment was then performed with a 10-ms laser irradiance pulse followed by mass isolation of the m/z 103 product ion. A series of MS^3 experiments on the m/z 103 ion performed by varying the laser irradiance times from 1 to 80 ms (increased energy input) produced the ion growth curve for the m/z 59 product ion shown in Figure 6. To verify the exclusive formation of the m/z 59 product ion from the m/z 103 parent, a second tandem mass spectrometry experiment was performed on the protonated diglyme parent ion (m/z 135) with concurrent notch-filter ejection of the m/z 103 product ion. As before, the laser irradiance time was varied from 1 to 80 ms. Results from this experiment produced only a decrease in the protonated diglyme parent ion, but no formation of the m/z 59 product ion. These experiments confirmed the formation of the m/z 59 product ion from the m/z 103 precursor, thus verifying the presence of consecutive reaction mechanism of the type m/z 135 $\rightarrow$ m/z 103 $\rightarrow$ m/z 59. The proposed mechanism of this consecutive reaction, seen in Figure 7, corresponds well to results reported previously for the IRMPD of protonated diglyme in the ICR cell [27].

The minimum number of photons (n) needed to reach the thermodynamic threshold for dissociation via a given reaction channel was calculated by dividing the enthalpy change by the photon energy:

$$\Delta H = nh\nu N_A \quad (1)$$

where ΔH is the enthalpy change, n is the number of photons absorbed, h is Planck's constant, ν is the

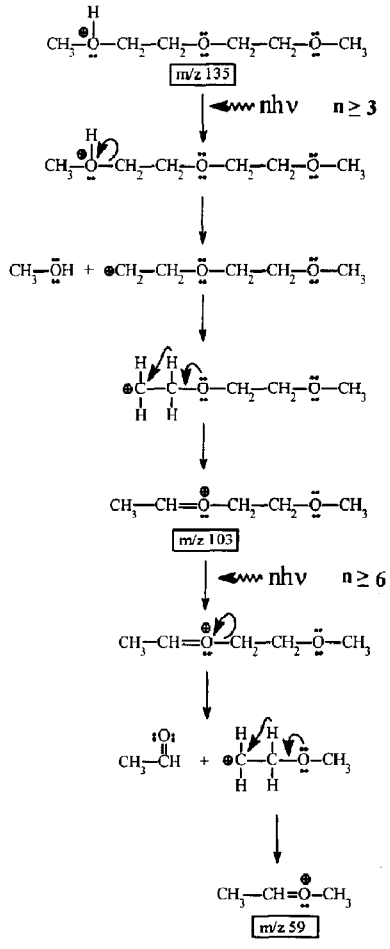

Figure 7. Photon absorption process and reaction mechanism of protonated diglyme.

frequency of the radiation used, and N_A is Avogadro's number. The ΔH_f values for neutral methanol, neutral acetaldehyde, and protonated diglyme were obtained directly from the literature [28]. The ΔH_f values for the photofragments m/z 103 and 59 were estimated by using quantum mechanical AM1 (Austin Model 1) calculations based on the neglect of diatomic differential overlap approximation [29, 30]. The accuracy of the AM1 calculations was checked by comparing the value obtained in the literature (114 kJ/mol) for protonated diglyme (m/z 135) against that of the AM1 routine (100 kJ/mol). A summary of the ΔH_f values for the two consecutive reactions of diglyme is given in Table 1. The errors observed in the tabulated values (e.g., ΔH_f $C_5H_{11}O_2^+$ and ΔH_f $C_3H_7O^+$) were on the order of 15 kJ/mol as determined by Katritzky et al. [31] for 14 different cationic species by using the AM1 calculation. The results obtained for the observed reaction channels were $n \geq 3$ for the lower energy process and $n \geq 6$ for the higher energy process as shown in

Table 1. Thermochemical data for the photodissociation of protonated diglyme

Reaction	$\Delta H_{f(reaction)}$ (kJ/mol)	$\Delta H_{f(products)}$ (kJ/mol)	$\Delta H_{f(reactions)}$ (kJ/mol)	Photons absorbed
$C_6H_{15}O_3^+ + nh\nu \rightarrow C_5H_{11}O_2^+ + CH_3OH$	37	$C_5H_{11}O_2^+ = 352^a$ $CH_3OH = -201^b$	$C_6H_{15}O_3^+ = 114^b$	$n \geq 3$
$C_5H_{11}O_2^+ + nh\nu \rightarrow C_3H_7O^+ + C_2H_4O$	68	$C_3H_7O^+ = 586^a$ $C_2H_4O = -166^b$	$C_5H_{11}O_2^+ = 352^a$	$n \geq 6$

[a] ΔH_f values obtained by AM1 calculations (refs 29 and 30).
[b] ΔH_f values obtained from ref 28.

Table 1. The total number of photons absorbed by the C—O stretches in protonated diglyme was $n \geq 9$ for formation of the m/z 59 fragment. The calculated photon energy at 944 cm^{-1} was 0.117 eV.

The photodissociation efficiency (P_D) for a given reaction is defined as the fraction of the original ion population photodissociated over a given exposure time (t) for a specified laser irradiance:

$$P_D = 1 - (I/I_0) \quad (2)$$

where I is the signal intensity of the dissociating ion (m/z 135 in this case) measured at the end of the exposure period and I_0 is the signal intensity after the same time period without irradiation. This definition of I_0 corrects for any unimolecular or collision-induced dissociation that may occur. Measurements for I_0 and I were an average of 10 consecutive analytical scans (laser off followed by laser on) with corresponding error bars in Figures 6, 8, 9, and 10 defined as the standard deviation of the mean. From eq 2, a first-order relationship for IRMPD kinetics was obtained:

$$\ln(I/I_0) = -k_D t \quad (3)$$

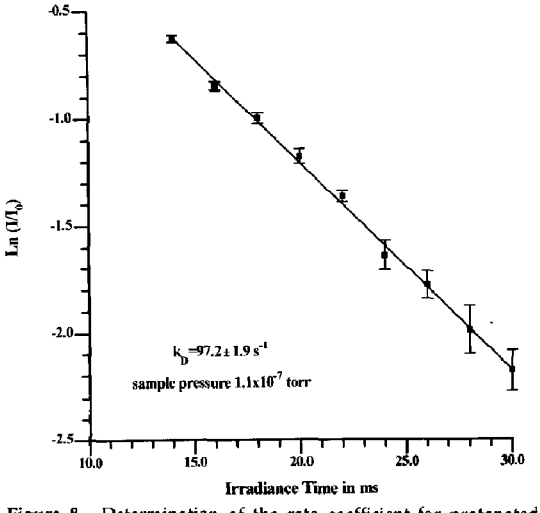

Figure 8. Determination of the rate coefficient for protonated diglyme at a pressure of 1.1×10^{-7} torr by using weighted linear regression, $k_D = 97.2 \pm 1.9\ s^{-1}$ (slope ± 95% confidence interval of the slope).

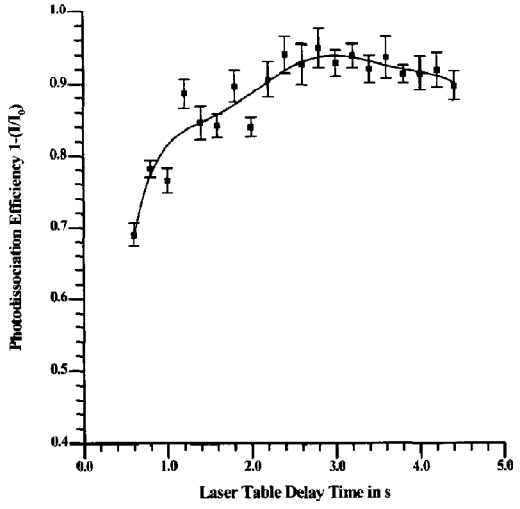

Figure 9. Photodissociation efficiency as a function of time after the He buffer gas pulse.

where k_D is defined as the photodissociation rate coefficient [12]. By plotting $\ln(I/I_0)$ versus t (Figure 8), the rate coefficient obtained for the diglyme $[M + H]^+$ ion was $k_D = 97.2 \pm 1.9\ s^{-1}$. This value was significantly higher than the 2–30-s^{-1} values obtained at higher laser irradiances reported in the literature [11, 12, 32]. Clearly the multipass ring electrode enhances photodissociation efficiency to a great extent. An investigation into the amount of photodissociation enhancement observed with the multipass design versus various single-pass designs is currently underway in our laboratory.

Pulsed valve experiments were conducted to determine if the increase in trapping efficiency during ionization associated with the addition of He buffer gas to the ion trap analyzer would interfere with the collision-free requirements subsequently needed for IRMPD. A 1.6-ms pulse of He gas was found to trap the maximum number of diglyme $[M + H]^+$ ions for a 10-psi He back pressure. The signal intensity of protonated diglyme (m/z 135) by using a 1.6-ms pulse of He gas during the pre-ionization period was higher by a factor of 7 than when He was not used in conjunction with the ionization event. The ionization time for both experiments was 1.0 ms.

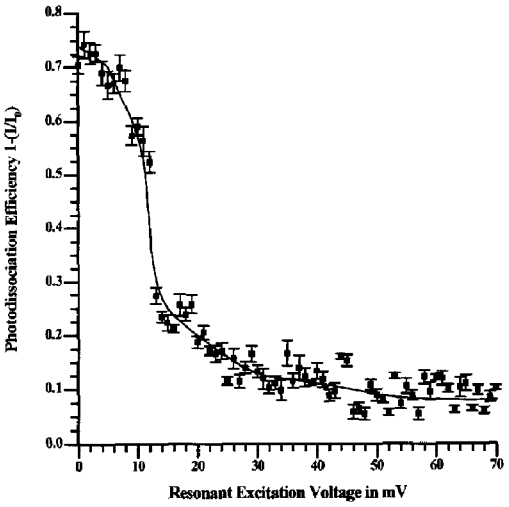

Figure 10. Effect of resonant excitation voltage on photodissociation efficiency of protonated diglyme.

For photodissociation to occur, the rate of photon absorption must be greater than that of collisional and radiative deactivation. Thus for pulsed-valve experiments, long ion storage times (several seconds) were required before triggering the laser to pump away the He buffer gas initially used to efficiently trap and damp the diglyme ions needed for the formation of the protonated (m/z 135) species. Storage efficiency measurements show an approximate loss of 2% of the original ion signal after 70 s of ion storage. The photodissociation efficiency as a function of the laser delay time is shown in Figure 9. After a 2-s delay between the He gas pulse and laser trigger, the photodissociation efficiency levels off at approximately 90%.

The multipass optical design used in these experiments produces a high photon density in the radial plane of the ring electrode as shown by Figure 2. A preliminary investigation to determine the influence of storage conditions (q_z and a_z) on photodissociation efficiency was undertaken with protonated diglyme. The effect on the photodissociation efficiency of exciting the $[M + H]^+$ ions of diglyme (no He present) by using resonant excitation (during period 5 in Figure 3) is seen in Figure 10. With increasing resonant excitation voltage applied to the endcaps, the axial excursions of the ions increase, thus the fraction of time the ions spend in the radial plane of the multipass ring electrode and therefore the extent of interaction between the stored ions and photons was decreased. This led to the decrease in photodissociation efficiency observed for increasing resonant excitation voltage.

Conclusions

The use of IRMPD in conjunction with ion trap mass spectrometry has been shown to be an effective tool for the study of fundamental gas-phase ion chemistry. By employing a multipass optical design, increased photodissociation efficiencies can be obtained for a variety of compounds in the IR region. This unique design allows for the determination of gaseous ion spectra and structural information for use with low power IR laser sources. The information obtained from determination of the dissociation pathway of lowest activation energy can aid greatly in the simplification of the structural elucidation process. Also, the use of a pulsed valve to increase the storage efficiency while obtaining ion populations under collision-free conditions, and for future use with ion injection, was demonstrated. The ability to store ions for long periods of time with minimal ion population loss allowed for the long irradiation periods necessary for MS^n experiments. Finally, the effect of resonant excitation voltage on photodissociation efficiency (e.g., ion residence time within the radial plane of the ring electrode) showed that even with a large optical path length, the axial excursions of the ions were important for efficient photodissociation.

Current and future investigations that involve the ion trap and photodissociation in our laboratory focus on four specific areas: (1) gas-phase ion chemistry studies with diglyme and other IR-absorbing compounds, (2) evaluation of various single-pass and multipass electrodes to determine the most efficient designs for photodissociation, (3) a detailed study of the ion trap stability diagram as it pertains to photodissociation efficiency that involves a given parent ion's a_z and q_z value, and finally (4) the use of matrix-assisted laser desorption and ion injection techniques for photodissociation (in the IR and UV–vis) of carbohydrate and glycoprotein molecules.

Acknowledgments

The authors thank the Office of Naval Research and the University of Florida Division of Sponsored Research for funding of this project, acknowledge Dr. Jie Coaxian for his assistance with the AM1 calculations, and recognize Dilrukshi Peiris, Ragulan Ramanathan, and Dr. Brad Coopersmith for their helpful discussions of gas-phase ion chemistry.

References

1. van der Hart, W. J. *Mass Spectrom. Rev.* **1989,** *8,* 237–268.
2. van der Hart, W. J. *Int. J. Mass Spectrom. Ion Processes* **1992,** *118 / 119,* 617–633.
3. Louris, J. N.; Brodbelt, J. S.; Cooks, R. G. *Int. J. Mass Spectrom. Ion Processes* **1987,** *75,* 345–352.
4. Mikami, N.; Miyata, Y.; Sato, S.; Saski, T. *Chem. Phys. Lett.* **1990,** *166,* 470–474.
5. Creaser, C. S.; McCoustra, M. R. S.; O'Neill, K. E. *Org. Mass Spectrom.* **1991,** *26,* 335–338.
6. Hemberger, P. H.; Nogar, N. S.; Williams, J. D.; Cooks, R. G.; Syka, J. E. P. *Chem. Phys. Lett.* **1992,** *191,* 405–410.
7. Morgenthaler, L. N.; Eyler, J. R. *J. Chem. Phys.* **1979,** *71,* 1486.
8. Moini, M.; Eyler, J. R. *Int. J. Mass Spectrom. Ion Processes* **1987,** *76,* 47–54.

9. Dunbar, R. C. In *Gas Phase Ion Chemistry*, Vol. 3: *Ions and Light*; Bowers, M. T., ed.; Academic Press: London, 1984; pp 130–164.
10. Busch, K. L.; Glish, G. L.; McLuckey, S. A. In *Mass Spectrometry / Mass Spectrometry: Techniques and Applications of Tandem Mass Spectrometry*; VCH: New York, 1988; pp 87-90.
11. Bomse, D. S.; Woodin, R. L.; Beauchamp, J. L. *J. Am. Chem. Soc.* **1979,** *101*, 5503–5512.
12. Thorne, L. R.; Beauchamp, J. L. In *Gas Phase Ion Chemistry*, Vol. 3: *Ions and Light*; Bowers, M. T., ed.; Academic Press: London, 1984; pp 41–97.
13. Hughes, R. J.; March, R. E.; Young, A. B. *Int. J. Mass Spectrom. Ion Phys.* **1982,** *42*, 255–263.
14. Hughes, R. J.; March, R. E.; Young, A. B. *Can. J. Chem.* **1983,** *61*, 834–845.
15. Hughes, R. J.; March, R. E.; Young, A. B. *Can. J. Chem.* **1983,** *61*, 824–833.
16. March, R. E.; Kamar, A.; Young, A. B. In *Advances in Mass Spectrometry 1985: Proceedings of the 10th International Mass Spectrometry Conference*; Wales, 1986; pp 949–950.
17. Kamar, A. Application of the Quadrupole Ion Storage Trap (QUISTOR) to the Study of Gas Phase Ion/Molecule Reactions, Ph.D. Thesis, Queens University, Kingston, Ont., Canada, 1985.
18. White, J. U. *J. Opt. Soc. Am.* **1942,** *32*, 285–288.
19. Watson, C. H.; Zimmerman, J. A.; Bruce, J. E.; Eyler, J. R. *J. Phys. Chem.* **1991,** *95*, 6081–6086.
20. Peiris, D. M.; Cheeseman, M. A.; Ramanathan, R.; Eyler, J. R. *J. Phys. Chem.* **1993,** *97*, 7839–7843.
21. ICMS Software, developed by Nathan A. Yates, Department of Chemistry, University of Florida.
22. Yates, N. A.; Yost, R. A. *Proceedings of the 39th ASMS Conference on Mass Spectrometry and Allied Topics*, Nashville, TN, May 19–24, 1991, p 1489.
23. Stafford, G. C.; Kelley, P. E.; Syka, J. E. P.; Reynolds, W. E.; Todd, J. F. J. *Int. J. Mass Spectrom. Ion Processes* **1984,** *60*, 85–98.
24. Weber-Grabau, M.; Kelley, P. E.; Bradshaw, S. C.; Hoekman, D. J. *Proceedings of the 36th ASMS Conference on Mass Spectrometry and Allied Topics*, San Francisco, CA, 1988, p 1106.
25. Basic, C.; Eyler, J. R.; Yost, R. A. *J. Am. Soc. Mass Spectrom.* **1992,** *3*, 716–726.
26. Bruce, J. E.; Eyler, J. R. *J. Am. Soc. Mass Spectrom.* **1992,** *3*, 727–733.
27. Baykut, G.; Watson, C. H.; Weller, R. R.; Eyler, J. R. *J. Am. Chem. Soc.* **1985,** *107*, 8036–8042.
28. Lias, S. G.; Bartmess, J. E.; Liebman, J. F.; Holmes, J. L.; Levin, R. D.; Mallard, W. G. *J. Phys. Chem. Ref. Data* **1988,** *17*, Suppl. 1, 74, 90, 274.
29. Dewar, M. J. S.; Zoebisch, E. G.; Healy, E. F.; Stewart, J. J. P. *J. Am. Chem. Soc.* **1985,** *107*, 3902.
30. Coaxian, J.; Stephenson, J. L. AM1 calculations, University of Florida.
31. Katritzky, A. R.; Watson, C. H.; Dega-Szafran, Z.; Eyler, J. R. *J. Am. Chem. Soc.* **1990,** *112*, 2476.
32. March, R. E.; Hughes R. J. In *Quadrupole Storage Mass Spectrometry*; Wiley: New York, 1989; pp 224–255.